

Alma Mater Studiorum Università di Bologna
Archivio istituzionale della ricerca

Multitarget Strategy to Address Alzheimer's Disease: Design, Synthesis, Biological Evaluation, and Computational Studies of Coumarin-Based Derivatives

This is the final peer-reviewed author's accepted manuscript (postprint) of the following publication:

Published Version:

Montanari, S., Bartolini, M., Neviani, P., Belluti, F., Gobbi, S., Pruccoli, L., et al. (2016). Multitarget Strategy to Address Alzheimer's Disease: Design, Synthesis, Biological Evaluation, and Computational Studies of Coumarin-Based Derivatives. CHEMMEDCHEM, 11(12), 1296-1308 [10.1002/cmdc.201500392].

Availability:

This version is available at: <https://hdl.handle.net/11585/549859> since: 2020-02-18

Published:

DOI: <http://doi.org/10.1002/cmdc.201500392>

Terms of use:

Some rights reserved. The terms and conditions for the reuse of this version of the manuscript are specified in the publishing policy. For all terms of use and more information see the publisher's website.

This item was downloaded from IRIS Università di Bologna (<https://cris.unibo.it/>).
When citing, please refer to the published version.

(Article begins on next page)

This is the final peer-reviewed accepted manuscript of:

Multitarget Strategy to Address Alzheimer's Disease: Design, Synthesis, Biological Evaluation, and Computational Studies of Coumarin-Based Derivatives

ChemMedChem 2016, 11, 1296–1308

The final published version is available online at:

<http://dx.doi.org/10.1002/cmdc.201500392>

Rights / License:

The terms and conditions for the reuse of this version of the manuscript are specified in the publishing policy. For all terms of use and more information see the publisher's website.

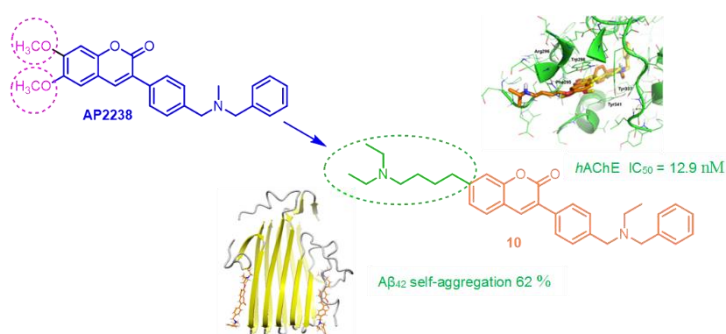
This item was downloaded from IRIS Università di Bologna (<https://cris.unibo.it/>)

When citing, please refer to the published version.

Table of Contents

Multi-target strategy to address Alzheimer's disease: design, synthesis, biological evaluation and computational studies of coumarin-based derivatives

Serena Montanari, Manuela Bartolini, Paolo Neviani, Federica Belluti, Silvia Gobbi, Letizia Pruccoli, Andrea Tarozzi, Federico Falchi, Vincenza Andrisano, Przemysław Miszta, Andrea Cavalli, Sławomir Filipek, Alessandra Bisi, Angela Rampa



Coumarin derivatives related to AP2238 were reported as disease modifying MTDLs in Alzheimer's disease. A small library of coumarin-based derivatives was designed and

synthesized, aimed at expanding the biological profile of the reference compound. Compound **10** emerged as nanomolar *hAChE* and significant Aβ₄₂ self-aggregation inhibitor, endowed with an additional promising neuroprotective behavior.

**MULTI-TARGET STRATEGY TO ADDRESS ALZHEIMER'S DISEASE: DESIGN,
SYNTHESIS, BIOLOGICAL EVALUATION AND COMPUTATIONAL STUDIES OF
COUMARIN-BASED DERIVATIVES**

Dr. Serena Montanari,^[a] Prof. Manuela Bartolini,^[a] Dr. Paolo Neviani,^[b] Dr. Federica Belluti,^[a]
Prof. Silvia Gobbi,^[a] Dr. Letizia Pruccoli,^[b] Prof. Andrea Tarozzi,^[b] Dr. Federico Falchi,^[c] Prof.
Vincenza Andrisano,^[b] Dr. Przemysław Misztal,^[d] Prof. Andrea Cavalli,^[a,c] Prof. Sławomir
Filipek,^[d] Prof. Alessandra Bisi,^[a] Dr. Angela Rampa^{*[a]}

^[a]*Department of Pharmacy and Biotechnology, Alma Mater Studiorum University of Bologna, Via
Belmeloro 6, 40126 Bologna, Italy.*

^[b]*Department for Life Quality Studies, Alma Mater Studiorum University of Bologna, Corso
d'Augusto 237, 47921 Rimini, Italy*

^[c]*CompuNet, Italian Institute of Technology, via Morego 30, 16163 Genova, Italy.*

^[d]*Faculty of Chemistry, Biological and Chemical Research Centre, University of Warsaw, Pasteura
1, 02093 Warsaw, Poland*

*Corresponding author:

Angela Rampa

Fax: +39 051 2099734

E-mail: angela.rampa@unibo.it

This item was downloaded from IRIS Università di Bologna (<https://cris.unibo.it/>)

When citing, please refer to the published version.

Abstracts

Alzheimer's disease represents a major public health challenge facing aging population worldwide. Current drug treatment has demonstrated only symptomatic efficacy, leaving an unmet medical need for a new generation of disease modifying therapies. Following the MTDLs approach, a small library of coumarin-based derivatives was designed and synthesized, as a follow-up of our studies on AP2238, aimed at expanding its biological profile. The coumarin substitution pattern in position 6 or 7 was modified by introducing alkyl chains of variable lengths and carrying different terminal amino functions. Compound **13**, bearing the bulkiest amine, emerged as a non-neurotoxic dual AChE/BuChE inhibitor, potentially suitable for the treatment of the middle stage of the disease. Besides, the introduction of a diethylamino spacer chain, as in compounds **4** and **10**, led to nanomolar *h*AChE inhibitors endowed with significant inhibition of A β ₄₂ self-aggregation, while the reference compound was completely ineffective. Compound **10** also showed a promising neuroprotective behavior, which makes it a potential candidate to be developed into a disease-modifying agent.

Keywords: Alzheimer's disease; A β ₄₂ inhibition; AChE; coumarin; MTDL.

This item was downloaded from IRIS Università di Bologna (<https://cris.unibo.it/>)

When citing, please refer to the published version.

Introduction

Alzheimer's disease (AD) is a neurodegenerative disorder of the brain that disrupts the thinking, language, behavioral and cognitive skills of a person. This kind of dementia is a major health issue predominantly affecting older people and, with ageing of world population, the number of patients suffering from AD is expected to dramatically increase in the future.^[1]

AD market is characterized by a lack of drugs with strong disease-modifying properties. Furthermore, a number of products failed in late stages of development over recent years. Indeed, current pharmacologic management is known to only provide temporary improvement of symptoms.

AD arises from the failure of synaptic transmission, which results in eventual death of the neurons present in specific areas of the brain. The cholinergic approach has been the first and the most frequently used therapeutic strategy for the treatment of mild to moderate AD. Levels of acetylcholine can be enhanced by inhibiting acetylcholinesterase (AChE), and four acetylcholinesterase inhibitors (AChEIs), namely tacrine (later withdrawn from the market due to its adverse effects), donepezil, rivastigmine and galantamine, have been approved by the FDA for the treatment of AD.^[2-3] In addition to targeting cholinergic deficiency, another strategy is to reduce glutamate-induced excitotoxicity by *N*-methyl-*D*-aspartate receptor antagonists, which led FDA to approve memantine.^[4]

Neuronal loss associated with AD leads to a reduction in brain size and to the deposition of debris from dead and dying neurons inside the brain. Moreover, key pathological features of AD are the formation of senile plaques (SPs)^[5] composed of extracellular deposits of β -amyloid ($A\beta$) peptides and the formation of neurofibrillary tangles (NFTs) inside the neuron cells.^[6]

This item was downloaded from IRIS Università di Bologna (<https://cris.unibo.it/>)

When citing, please refer to the published version.

The temporal profile of pathological features together with genetic risk factors for AD have led to the hypothesis that accumulation of A β oligomers during early, preclinical stages of the disease initiates a cascade of events resulting in synaptic dysfunction and neural loss which lead to a progressive cognitive impairment.

The different isoforms of A β , the main constituent of the SPs, are produced by proteolytic cleavage from a larger precursor molecule called Amyloid Precursor Protein (APP), a ubiquitous integral membrane protein, which can undergo proteolytic processing by two distinct pathways: the ‘non-amyloidogenic’ and the ‘amyloidogenic’ pathway. The amyloidogenic one is an alternative cleavage pathway for APP, mediated by two enzymes, β - and γ -secretase.^[7] This cleavage predominantly produces A β ₄₀ (the 40-aminoacid long isoform) and A β ₄₂ (the 42-aminoacid long isoform) at a ratio of 10:1. A β ₄₂ peptide is more hydrophobic and prone to form aggregates than the shorter isoforms. Its self-association is known to be crucial for the A β -associated neurotoxic effects observed in AD brain, as stated in the so called amyloid hypothesis.^[8]

The aggregation of A β peptides is a nucleation-elongation process, which is initiated by monomer misfolding. Progressively, A β self-assembly generates various types of assemblies including oligomers, protofibrils and finally amyloid fibrils, which deposit into senile plaques. The precise molecular nature of the neurotoxic species and the mechanism of toxicity is still under debate.

However, increasing evidence in last few years indicates soluble oligomers as the primary neurotoxic species^[7,9] which trigger multiple neurotoxic/synaptotoxic mechanisms *in vitro* and *in vivo*, resulting in impaired cognition. Thus, even if the predominant role is still controversial, it is acknowledged that levels of high molecular weight oligomers are increased in the cerebrospinal fluid (CSF) of AD patients^[10] and in AD brain.^[11] The toxic role played by amyloid soluble aggregates has recently received further support from the promising results obtained in Phase I

This item was downloaded from IRIS Università di Bologna (<https://cris.unibo.it/>)

When citing, please refer to the published version.

clinical trials with the recombinant antibody Aducanumab (BIIB037), which targets aggregated forms of A β , both plaques and soluble oligomers, but not monomers (clinical trials identifier NCT01397539).

Therefore, interfering with the overall A β aggregation process with small molecules could represent an important strategy in the development of effective anti-AD therapeutic approaches.

Taken together, these remarks underline the multifaceted and heterogeneous nature of AD, and consequently drugs designed to act against individual molecular target may not be the best choice to effectively combat this complex disease. Indeed, the “single-target” approach for the treatment of AD, in analogy to other multifactorial disorders, has shown several limitations. The ‘multi-target-directed ligand’ (MTDL) strategy is based on the concept that a single molecular entity can be designed to hit multiple targets that cooperate in the network of the disease, and this paradigm has been the focus of researchers’ increasing attention over the last decade.^[12-14]

Our research group has been involved for several years in the development of MTDLs and in the past we purposely designed compound **1** (AP2238, Figure 1) with the aim to bind both central and peripheral anionic sites of the human acetylcholinesterase (*hAChE*), linking a *N,N*-methylbenzylamino group and a coumarin heterocycle through a phenyl ring.^[15] The combined molecule turned out to be the first compound to allow the simultaneous inhibition of both the catalytic and the A β pro-aggregating activities of the *hAChE*. Extensive SAR studies^[16] showed that all the structural elements in the lead compound **1** were crucial for optimal activities, since only a slight modification of **1** was tolerated. Compound **2** (AP2243, Figure 1), which carried an ethyl instead of a methyl group on the basic nitrogen, led to an improvement in both catalytic and A β aggregation activities. In this paper, we further modified the coumarin substitution pattern (i.e., the methoxy groups of **2**) by introducing alkyl chains of various lengths, carrying different amino

This item was downloaded from IRIS Università di Bologna (<https://cris.unibo.it/>)

When citing, please refer to the published version.

functions at the end, in positions 6 or 7 of the coumarin core. The side chain increases the overall size of the molecule, possibly leading to additional interactions with A β , and moreover, the amino functions could establish hydrogen bonds with the amidic backbone of A β , which may stabilize the non amyloidogenic conformation (unordered/ α). In summary, a small library of 11 new derivatives was synthesized, whose structures are collected in Table 1.

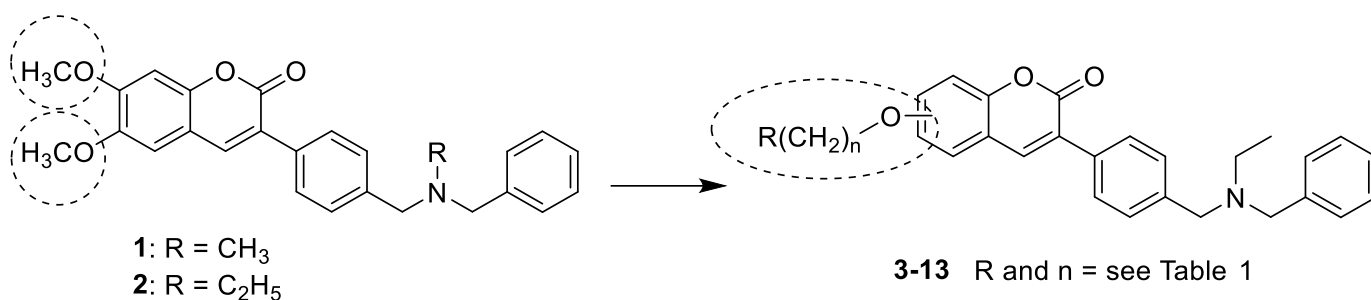


Figure 1. Structures of the lead compounds (**1** and **2**) and of the newly-synthesized coumarin derivatives (**3-13**).

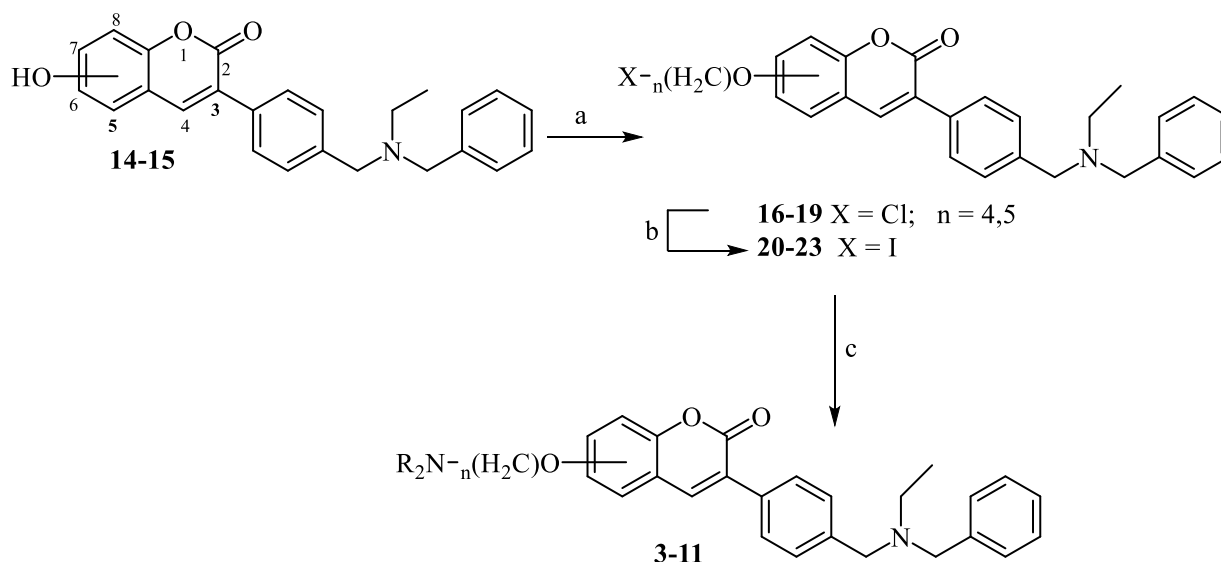
Chemistry

The synthesis of the studied compounds was accomplished as shown in Scheme 1. Previously described 3-(4-((benzyl(ethyl)amino)methyl)phenyl)-6-hydroxy-2*H*-chromen-2-one (**14**)^[17] or 3-(4-((benzyl(ethyl)amino)methyl)phenyl)-7-hydroxy-2*H*-chromen-2-one (**15**)^[17] were alkylated with the selected 1-bromo- ω -chloroalkane, in the presence of K₂CO₃, to afford the chloroalkoxy derivatives **16-19**. Then, these compounds were reacted with NaI to obtain the more reactive iodinated analogues (**20-23**), which were subjected to nucleophilic attack by selected amines via a parallel synthesis procedure. Purification of each crude product by flash column chromatography yielded the desired final compounds **3-11**.

This item was downloaded from IRIS Università di Bologna (<https://cris.unibo.it/>)

When citing, please refer to the published version.

Scheme 1. "Synthesis of compounds **3-11**.



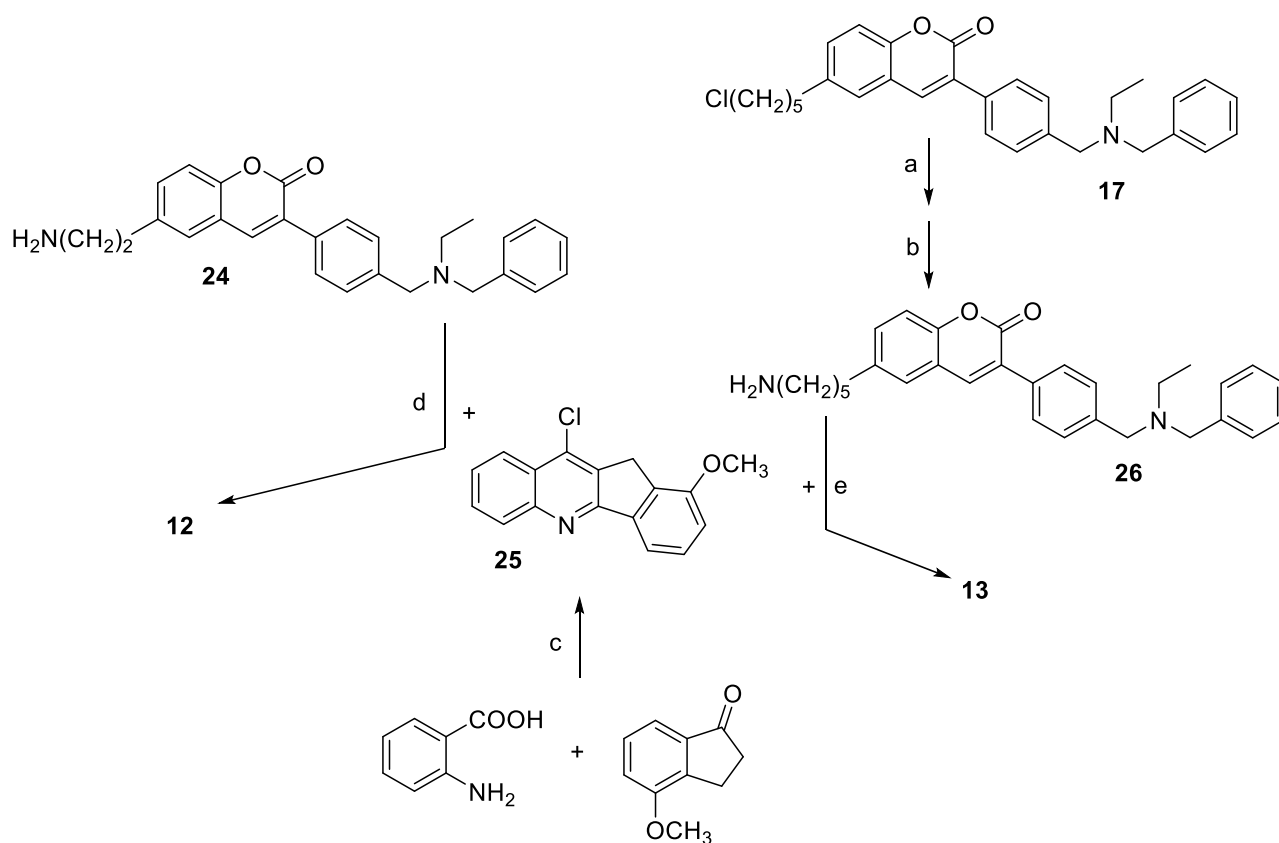
Reagents and conditions: a) $Cl(CH_2)_nBr$, K_2CO_3 , reflux; b) NaI , $MeCOEt$, reflux; c) R_2NH , toluene, reflux.

In Scheme 2 the synthesis of derivatives **12-13** was illustrated. Compound **17** was turned into a primary amine using Gabriel's procedure. In particular, after obtaining the phthalic end, the intermediate was converted in **26** using hydrazine. Aromatic substitution of **26** with **25**, previously obtained by reacting anthranilic acid with 4-methoxyindanone in $POCl_3$, afforded compound **13**. In a similar way, by reacting intermediates **24**^[17] and **25**, **12** was obtained.

Scheme 2. "Synthesis of compounds **12-13**.

This item was downloaded from IRIS Università di Bologna (<https://cris.unibo.it/>)

When citing, please refer to the published version.



“Reagents and conditions: a) potassium phthalimide, DMF, reflux; b) hydrazine monohydrate, EtOH, reflux, then HCl; c) POCl_3 , reflux; d) PhOH, 130 °C; e) 1-pentanol, 180 °C.

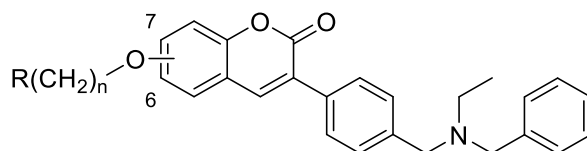
Results and discussion

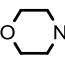
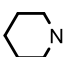
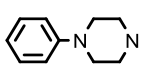
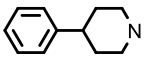
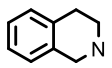
The inhibitory activities against both recombinant human AChE and BuChE from human serum of the newly synthesized compounds were evaluated using the method described by Ellman.^[18] The results, together with those of AP2243 (**2**) and donepezil taken as references, are reported in Table 1, and are expressed as IC_{50} values.

This item was downloaded from IRIS Università di Bologna (<https://cris.unibo.it/>)

When citing, please refer to the published version.

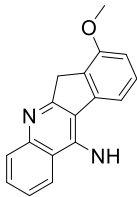
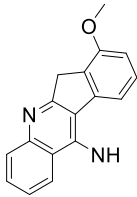
Table 1. Inhibitory activities on *hAChE*, *hBuChE* and A β ₄₂ self-aggregation and neurotoxicity of the studied compounds.



Comp.	n	R	Chain position	IC ₅₀ (nM) ± SEM <i>hAChE</i>	IC ₅₀ (nM) ± SEM <i>hBuChE</i>	Inhibition (%) ± SEM A β ₄₂ self-aggregation	IC ₅₀ (μM) ± SD Neurotoxicity
2	-	-	-	18 ± 3 ^a	118000 ± 16000	< 5	> 40
3	4	NEt ₂	6	30.5 ± 6.2	3870 ± 240	10.3 ± 5.5	nt
4	5	NEt ₂	6	11.7 ± 1.2	4290 ± 160	56.4 ± 4.9	19.1 ± 2.8
5	5		6	131 ± 12	na ^b	nt	> 40
6	5		6	27.3 ± 2.5	8540 ± 390	15.4 ± 5.1	22.6 ± 3.4
7	5		6	4610 ± 580	na ^b	nt	> 40
8	5		6	1960 ± 160	75600 ± 11100	nt	nt
9	5		6	468 ± 14	>>10	nt	> 40

This item was downloaded from IRIS Università di Bologna (<https://cris.unibo.it/>)

When citing, please refer to the published version.

10	4	NEt ₂	7	12.9 ± 0.7	7210 ± 250	62.0 ± 3.4	16.4 ± 2.4
11	5	NEt ₂	7	11.1 ± 1.2	4920 ± 170	59.2 ± 1.5	nt
12	2		6	3510 ± 130	23000 ± 2500	nt	> 40
13	5		6	653 ± 55	783 ± 65	nt	nt
donepezil	-	-	-	23.1 ± 4.8	7420 ± 390	<10	nt

^afrom ref.^[16]; ^bnot active at the highest tested concentration i.e. 30 µM; nt stands for not tested.

Values are expressed as mean ± standard error of the mean (SEM) of at least three experiments (n=3), each performed in duplicate.

To assess the importance of the diethylamino spacer chain inserted in position 6 or 7 on the coumarin core, its length was varied from four to five methylene units to obtain compounds **3** and **10** (n = 4), and **4** and **11** (n = 5), respectively. The positioning of this side chain proved not to be relevant for anti-AChE activity, as all these compounds showed potencies in the nanomolar range, turning out to be the most potent in the series. Considering that derivative **4** was slightly more potent than **3** (IC₅₀=11.7 nM and 30.5 nM, respectively), the spacer was maintained in position 6 and its length was settled to five methylene units for the following set of synthesized molecules. In this context, the role of the diethylamino moiety itself was evaluated by generating a series of derivatives in which this function was substituted with different cyclic amino functions. The introduction of a piperidine (to obtain compound **6**) allowed maintaining good activity on AChE,

This item was downloaded from IRIS Università di Bologna (<https://cris.unibo.it/>)

When citing, please refer to the published version.

while its replacement with a morpholine group (compound **5**) led to a fivefold decrease in potency. With the introduction of bulkier amines, as phenylpiperazine (**7**), phenylpiperidine (**8**) and 1,2,3,4-tetrahydroisoquinoline (**9**), an unexpected loss in activity on AChE was noticed.

To understand the mode of interaction and define the SAR profile, all compounds were docked into the crystal structure of *hAChE* (PDB code 4EY7^[19]) with the Glide software (Schrodinger Suite 2014-3^[20]). From these studies all the compounds seem to share the same binding mode, where the coumarin framework is embedded within the protein core and both the amine and the spacer chain are solvent exposed (Figure 2, 3 and 4). Notably, all the compounds showed comparable docking scores.

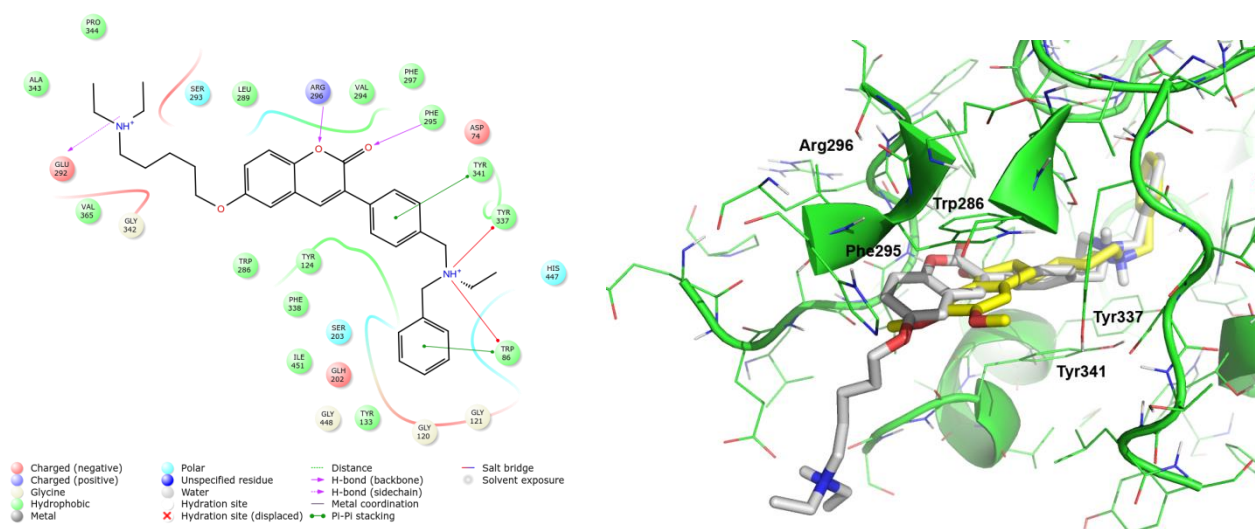


Figure 2. A 2D ligand interaction diagram of **4** is shown at left. Binding mode of **4** (grey) with respect to donepezil (yellow) is shown at right.

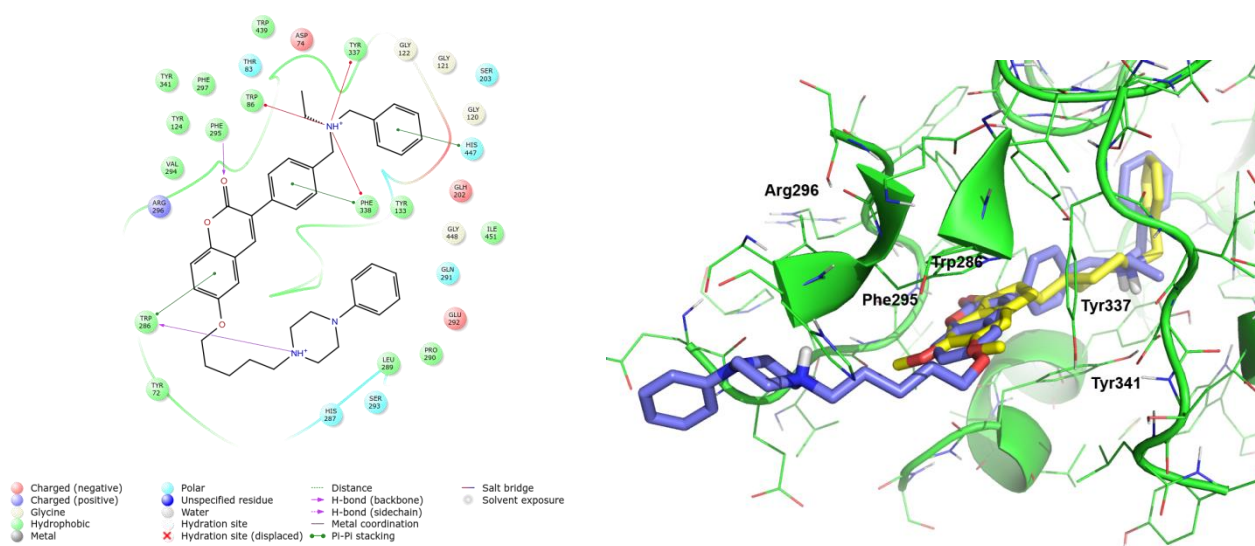


Figure 3. A 2D ligand interaction diagram of **7** is shown at left. Binding mode of **7** (blue) with respect to donepezil (yellow) is shown at right.

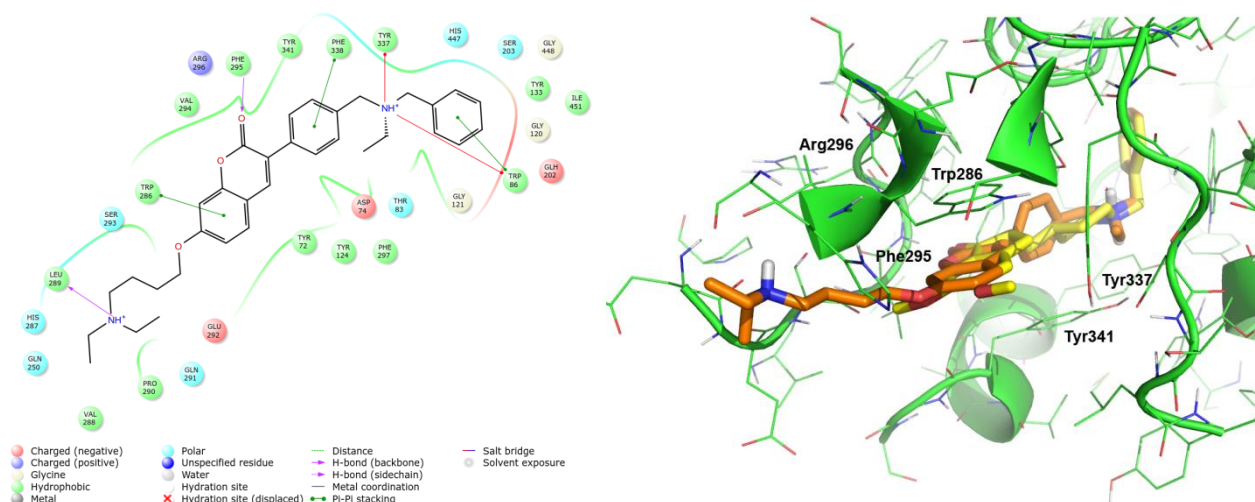


Figure 4. A 2D ligand interaction diagram of **10** is shown at left. Binding mode of **10** (orange) with respect to donepezil (yellow) is shown at right.

This item was downloaded from IRIS Università di Bologna (<https://cris.unibo.it/>)

When citing, please refer to the published version.

In order to gain insight into this different AChE inhibitory profile, a molecular dynamics (MD) simulation of the most and the least potent derivatives (**4** and **7**, respectively) was performed. As shown in Figure 5, the RMSD of the solvent exposed portion of **7** was significantly higher than that of **4** and, therefore, it can be concluded that the solvent exposed portion of **7** was more unstable than the corresponding portion of **4**, as could be expected for the presence of the highly hydrophobic aromatic portion in **7**. Moreover, the higher flexibility of the solvent exposed portion induces a higher flexibility in the protein bound portion (see Figures 2 and 3), thus destabilizing the binding mode and causing a loss of potency.

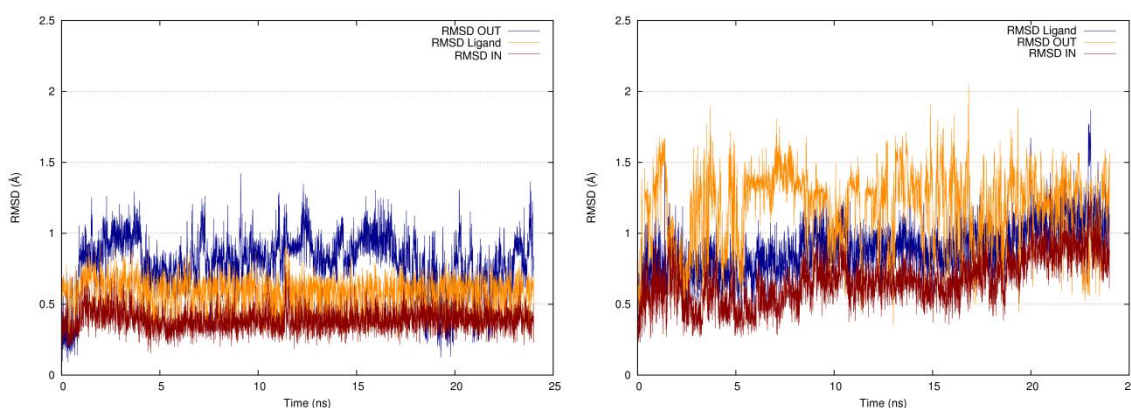


Figure 5. RMSD of **4** is shown at left. RMSD of **7** is shown at right. “*RMSD in*” is the RMSD of the portion of the ligand inside the protein; “*RMSD out*” is the RMSD of the portion of the ligand solvent exposed; “*RMSD ligand*” is the RMSD of the whole ligand.

Finally, a 7-methoxy-6*H*-indeno[2,1-*b*]quinolin-11-amino moiety, described as AChE inhibitor in our previous papers,^[21-22] was introduced. The choice of this group was due to the fact that, in previously studied molecules, the introduction of a methoxy group on this tetracyclic nucleus exerted a detrimental steric effect making those compounds unable (at all or in part) to penetrate

inside the AChE active site gorge. Therefore, the idea was here to drive the entry of the molecule from the benzylaminic side, leaving the bulky aminic group outside the gorge, to assess the appropriate chain length to reach the active site and the possible additional interactions of this rigid and bulky moiety. The spacer chain was kept to five methylene units (compound **13**) or shortened to two (compound **12**). In this case, the shorter chain was selected considering the plausible partial entrance of this polycyclic moiety into the AChE gorge, that could counteract the lack of three methylene units. The inhibitory potencies of these analogues confirmed that when a bulky substituent was introduced, the length of the spacer played a key role in maintaining a good inhibitory activity. Indeed, a short chain conferred to **12** a micromolar activity (3.51 μM), while the introduction of a longer chain led to a 5.4-fold more active derivative (compound **13**).

The AChE/BuChE selectivity was investigated by measuring the inhibitory activity on BuChE from human serum. All compounds were weak BuChE inhibitors, with IC_{50} values mostly in the micromolar range (from 0.87 μM to 75.6 μM , excluding **13**) and were thus highly AChE-selective. Derivative **13**, bearing a five-methylene spaced bulky substituent in position 6, showed a comparable low-micromolar activity on both enzymes. Some considerations can be made on the different selectivity and activity profiles of **13** and **4**, principally related to the different size of their amino functions and that of the entrance of the catalytic gorge in the two enzymes. Indeed, the active gorge is larger in *h*BuChE than in *h*AChE. The *h*AChE active site is lined by 14 aromatic residues, and six of them are replaced by smaller aliphatic residues in *h*BuChE. In particular, the replacement of two phenylalanine residues by the smaller amino acids valine and leucine makes the acyl pocket larger and enables bulkier molecules to better fit into the gorge.^[23]

Aiming at assessing the multifunctional profile of the compounds, the anti-aggregating properties of the five most active cholinesterase inhibitors were evaluated *in vitro* by a Thioflavin T (ThT)-based

This item was downloaded from IRIS Università di Bologna (<https://cris.unibo.it/>)

When citing, please refer to the published version.

assay^[24] and the results were reported in Table 1. Indeed, while the dimethoxy lead **2** was previously shown to be inactive as inhibitor of amyloid self-aggregation,^[16] compounds **4**, **10** and **11**, all containing diethylamine moiety, proved to significantly inhibit A β ₄₂ self-aggregation to a similar extent (from 56.4% to 62.0% at 1/1 ratio with A β ₄₂). On the other hand, the inclusion of the amino function into a cyclic ring showed a detrimental effect on the inhibitory properties. Indeed derivative **6**, bearing a piperidine function, resulted almost inactive (inhibition = 15.4%) when tested at 1/1 ratio with A β ₄₂. Worth to note and unexpectedly, compound **3**, bearing a four methylene spacer chain in position 6 of the coumarin moiety, proved to be a significantly weaker inhibitor than both derivative **4**, which bears a 1-methylene longer spacer chain (10.3% vs 54.6%) and compound **10**, carrying the same 4-carbon spacer chain in position 7 instead of 6 (10.3% vs 62.0%). Thus, due to the similarity of the chemical structures of these derivatives, it was conceivable to conclude that the relative position of key interacting moieties is crucial for an optimal inhibition and it became of high interest to get further insights into the structural features required for a good interaction with amyloid oligomers. To this aim, MD simulations were carried out to highlight the interaction between derivatives **3**, **4** and **10** and A β ₄₂ protofibrils.

As it was seen from 600 ns MD simulations, the amyloid A β ₄₂ (five monomers A-E) is forming a stable protofibril which is twisted about 27° (Figure 6). The starting structure, based on NMR data (PDB id:2BEG), is not twisted at all, therefore, it was important to compare obtained results of simulations with ligands to equilibrated structure of protofibril which should be naturally twisted as seen in other molecular structures composed of β -sheets. *N*-terminus of A β ₄₂, comprising of residues 1-15, is mostly disordered apart from monomer E which is forming a β -sheet in a paperclip shape while disordered *N*-terminus from monomer A contains more residues 1-19. It indicates an inclination to extend fibril from one end (monomer E).

This item was downloaded from IRIS Università di Bologna (<https://cris.unibo.it/>)

When citing, please refer to the published version.



Figure 6. Structure of fragment of protofibril composed of five amyloid monomers after 600 ns of MD simulation. The protofibril got twisted by about 27°. N-terminus from one end (monomer E) formed a β -sheet in a paperclip shape. N-termini of other monomers are mostly disordered. In the right panel, the structure after rotation by 90°.

Derivative **3** makes the protofibril wider and in consequence it mostly interacts mostly with only one part of β -sheet of A β ₄₂ in a similar way at side A and E (Figure 7). Twisting of protofibril is smaller than that without a ligand and amounts about 18°. The residues in vicinity of 2.5 Å around a ligand: 15 at side E (residues E₃V₁₂F₁₆ from monomer D, and D₇G₉Y₁₀H₁₄Q₁₅F₁₆F₁₉F₂₀E₂₂V₂₄L₃₄A₄₂ from monomer E) and 16 at side A (E₃F₄R₅H₆Y₁₀V₁₂F₁₆L₁₇V₁₈F₂₀ from monomer A, and D₁E₃G₉Y₁₀V₁₂F₂₀ from monomer B). The large number of interacting residues is a consequence of binding to N-termini of not only flanking monomers (A, E) but also of adjacent ones (B, D). N-termini are mostly disordered and can wrap around the ligand. The second consequence of such

binding is interacting with only one part of folded β -sheet so the second part is free and can recruit an additional monomer of amyloid.

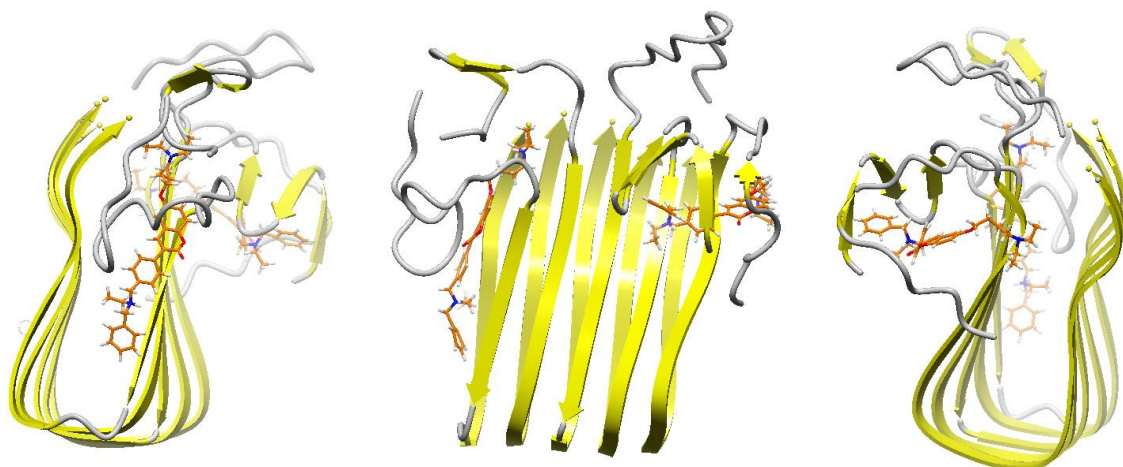


Figure 7. Structure of fragment of protofibril interacting with two copies of compound **3** at both ends of protofibril after 600 ns of MD simulation. The ligands are interacting mainly with N-termini and only one part of β -sheet of amyloid. All panels are showing the same structure after rotating by 90° . Left panel – side E, right panel – side A.

In the case of compound **4** the fibril twisting is about 23° . The ligand interacts with 9 residues of $A\beta_{42}$ in 2.5 \AA vicinity of the ligand at side E (A_{21} from monomer D, and $E_{11}H_{14}A_{21}D_{23}L_{34}V_{36}V_{39}I_{41}$ from monomer E), and with 10 residues at side A ($F_{16}L_{17}F_{19}G_{25}G_{29}V_{36}G_{38}$ from monomer A, and $K_{28}V_{36}G_{38}$ from monomer B). At side E, the ligand is covered by *N*-terminal residues forming a paperclip fold and the ligand is nearly entering the interior of protofibril (Figure 8). One part of folded β -sheet is composed of residues 17-27 while the second one of residues 29-42 so the ligand

at side E interacts with 3 residues of first part of β -sheet and with 4 residues of the second part. The ligand at side A interacts similarly and forms 6 interaction with both parts of β -sheet (3+3).

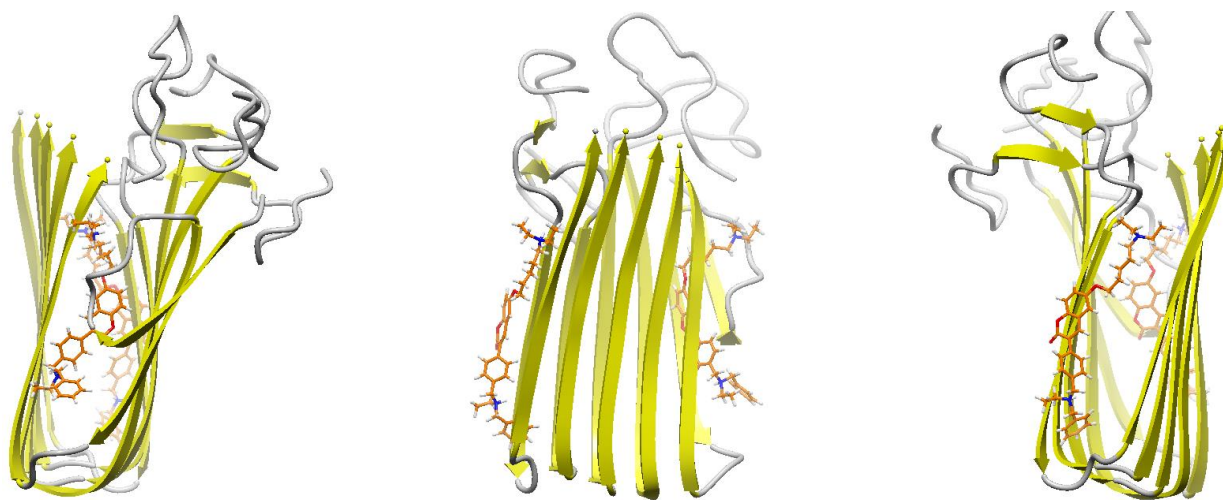


Figure 8. Structure of fragment of protofibril interacting with two copies of compound **4** at both ends of protofibril after 600 ns of MD simulation. The ligand is interacting with both parts of folded β -sheet of amyloid. All panels are showing the same structure after rotating by 90° . Left panel – side E, right panel – side A.

Finally, in case of compound **10**, similarly to compound **4**, the protofibril is also not wide in the bottom part as it is the case for compound **3**, and the ligand can bind to both parts of β -sheet of $A\beta_{42}$ (Figure 9). Twisting of protofibril is about 32° . The ligand **10** interacts with 9 residues of $A\beta_{42}$ in 2.5 \AA vicinity of the ligand at side E ($G_9Y_{10}A_{21}E_{22}D_{23}S_{26}N_{27}K_{28}V_{36}$ all from monomer E), and with 14 residues at side A ($D_1A_2E_3F_4R_5D_7V_{18}F_{19}F_{20}A_{21}D_{23}G_{29}A_{30}$ from monomer A, and E_3 from monomer B). Such a large number of interacting residues (similar to compound **3**) at side A comes

from interactions with disordered *N*-terminus, however, both parts of folded β -sheet are involved, and the ligand is located centrally at the axis of fibril.

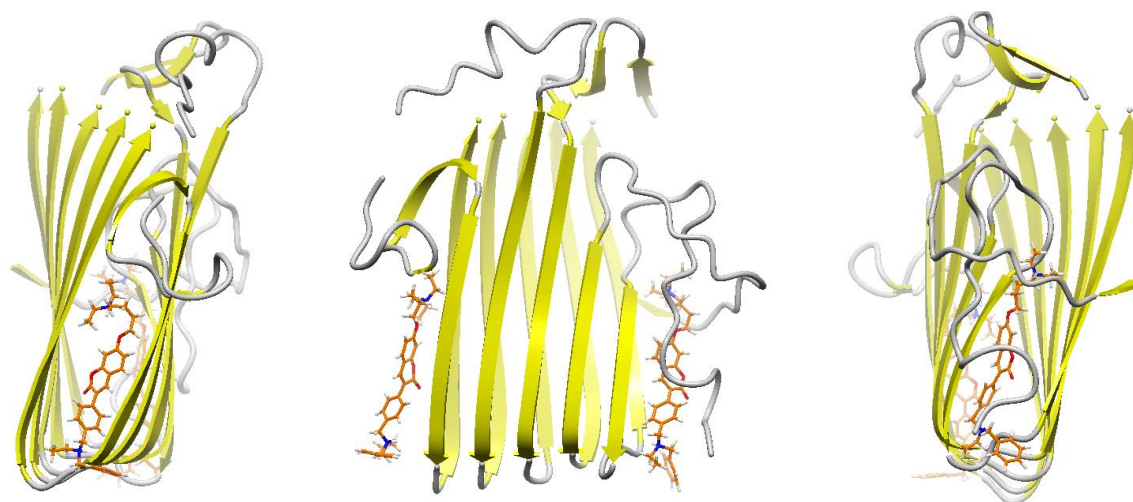


Figure 9. Structure of fragment of protofibril interacting with two copies of compound **10** at both ends of protofibril after 600 ns of MD simulation. The ligand, similarly to ligand **4**, is interacting with both parts of β -sheet of amyloid. All panels are showing the same structure after rotating by 90°. Left panel – side E, right panel – side A.

In summary, blocking of protofibril is effective only when both parts of the β -sheet of amyloid are engaged in binding to the ligand and the ligand is bound more or less centrally on the fibril axis.

Although the compound **3** interacts with a larger number of residues of A β ₄₂ than for more active compounds **4** and **10**, those residues are mainly from *N*-termini and the ligand is relocated outside the center of the protofibril. The other compounds, **4** and **10**, are located centrally at the axis of the fibril so they can effectively block the binding of additional monomers of amyloid.

Acute neurotoxicity elicited by compounds **2**, **4-7**, **9**, **10** and **12** [1.25 - 40 μ M] in human neuronal SH-SY5Y cells was in parallel investigated using a colorimetric MTT assay. As shown in Table 1,

This item was downloaded from IRIS Università di Bologna (<https://cris.unibo.it/>)

When citing, please refer to the published version.

compounds **4**, **6** and **10** were more neurotoxic than compounds **2**, **5**, **7**, **9** and **12**. Interestingly, the introduction of diethylamine and piperidine group increase the ability of compounds **4**, **6** and **10** to interact with *hAChE* and $A\beta_{42}$ as well as to exert neurotoxicity. These results could suggest that the amino acid targets present in *hAChE* and $A\beta_{42}$ could also play a role in survival of neuron cells.

The good ability of **4** and **10** to interfere with the aggregation processes of $A\beta_{42}$ made these compounds eligible for further experiments aimed at assessing their neuroprotective potential against the neurotoxicity elicited by $A\beta_{42}$ oligomers.

In this regard, SH-SY5Y cells were treated with compounds **4** and **10** [1 μ M] in the presence of $A\beta_{42}$ oligomers [10 μ M] and neurotoxicity induced by $A\beta_{42}$ oligomers was then evaluated by MTT assay. Compound **10**, but not **4**, significantly decreased $A\beta_{42}$ oligomers-induced neurotoxicity with a maximum of inhibition of 25% (Figure 10). Regarding this evidence, it could be plausible that both the length of the diethylamino spacer chain and its position on the coumarin core improve the ability of compound **10** to block the interaction between the $A\beta_{42}$ oligomers and the neuronal plasma membrane, a toxic event leading to neuronal death.^[25] In this regard compound **10**, having a structure composed of aromatic rings, appeared to be quite suitable for specific interactions with the aromatic residues of $A\beta_{42}$ peptide,^[26,27] as confirmed by MD studies and in agreement with *in vitro* antiaggregating activity data.

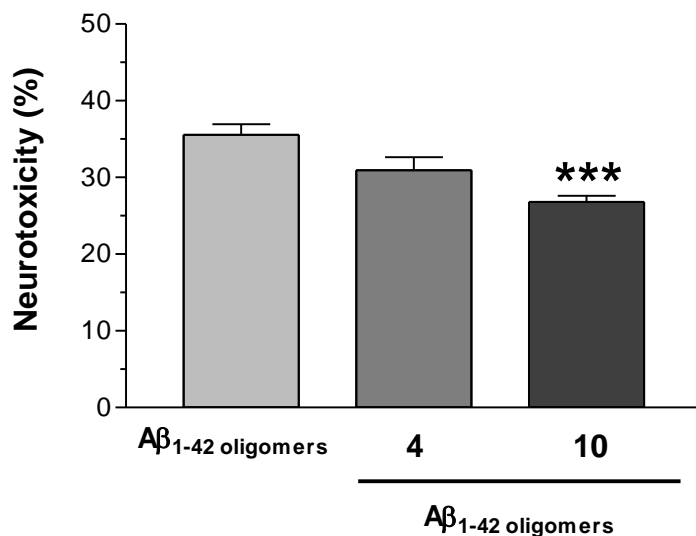


Figure 10. Effects of compounds **4** and **10** on Aβ₄₂ oligomer-induced neurotoxicity in SHSY-5Y cells. The neurotoxicity was determined by MTT assay (as described in the Experimental section), after 24 h of treatment with Aβ₄₂ oligomers [10 μM] in the presence of compounds [1 μM]. The results are expressed as a percentage of control cells and the values are reported as mean ± SD of three independent experiments (***) p<0.001 vs treated cells with Aβ₄₂ oligomers; t-test).

Finally, the results on neuroprotection suggested a good therapeutic window for compound **10** which has a fivefold difference in the neuroprotective concentration (1 μM) and minimum neurotoxic concentration (5 μM).

As selected targets are located in the CNS, the ability of the most active compounds **4** and **10** to penetrate the blood–brain barrier (BBB) was also estimated by calculating their physico-chemical properties. In particular, even if the logP value is slightly above 5, having a number of hydrogen bond donors ≤3 (n. H-bond donor = 0), number of hydrogen bond acceptors ≤7 (n. H-bond acceptors = 5), and molecular weight close to 500 g/mol (525 g/mol for **4** and 511 g/mol for **10**), the

This item was downloaded from IRIS Università di Bologna (<https://cris.unibo.it/>)

When citing, please refer to the published version.

selected compounds appeared in reasonable agreement with Lipinski's and Wenlock's guidelines for good passive CNS penetration.^[28,29]

Conclusions

Due to the multifactorial nature of AD, molecules that modulate the activity of a single protein target are unable to significantly modify the progression of the disease. The researchers are now turning to the design of structures that should be able to simultaneously interact with different targets. Following this new paradigm, here we have reported a new series of coumarin-based derivatives, related to the previously described potent AChE inhibitor AP2243 (**2**), endowed with a multipotent profile. Compound **13**, bearing a tetracyclic nucleus at the end of the spacer, turned out to inhibit both human AChE and BuChE enzymes with a well-balanced submicromolar potency. This dual activity, together with the lack of neurotoxicity, makes this compound potentially suitable for the treatment of early to moderate (middle-stage) forms of the disease.

Significantly, the introduction of the diethylamino spacer chain in positions 6 or 7 on the coumarin core led to an improved potency on *h*AChE inhibition with respect to our lead compound **2** and the marketed drug donepezil, and to a significant reduction in A β ₄₂ self-aggregation. Interesting hits proved to be compounds **4** and **10**, with inhibitory activities of *h*AChE in the nanomolar range and the ability to reduce A β ₄₂ aggregation of about 60%. In addition, compound **10** was able to block the neurotoxic effects induced by preformed A β ₄₂ oligomers, showing a promising neuroprotective behaviour, which makes this compound a potential disease-modifying agent.

Experimental section

This item was downloaded from IRIS Università di Bologna (<https://cris.unibo.it/>)

When citing, please refer to the published version.

Chemistry. General Methods. Starting materials, unless otherwise specified in the Experimental Section, were used as high-grade commercial products. Solvents were of analytical grade. Melting points were measured in glass capillary tubes on a Büchi SMP-20 apparatus and are uncorrected. Direct infusion ES-MS spectra were recorded on a Waters Micromass ZQ 4000 apparatus. ^1H NMR and ^{13}C NMR spectra were recorded in CDCl_3 solution on a Varian Gemini 300/400 MHz spectrometer. Chemical shifts are reported in parts per million (ppm) relative to tetramethylsilane (TMS), and spin multiplicities are given as s (singlet), d (doublet), t (triplet), m (multiplet) or br (broad). Reaction courses were followed by thin layer chromatography (TLC) on precoated silica gel plates (Merck Silica Gel 60 F254) and then visualized with a UV lamp. Chromatographic separations were performed on silica gel columns (Kieselgel 40, 0.040-0.063 mm; Merck) by flash chromatography. Chemical purities of the tested compounds were determined by elemental analysis (C, H, N) and were within ± 0.4 % of the theoretical values. Compounds were named following IUPAC rules as applied by Beilstein-Institut AutoNom (version 2.1), a PC integrated software package for systematic names in organic chemistry.

3-(4-((benzyl(ethyl)amino)methyl)phenyl)-6-(4-chlorobutoxy)-2H-chromen-2-one (16). A stirred mixture of **14** (1.07 g, 2.78 mmol), 1-bromo-4-chloroethane (0.48 mL, 4.17 mmol) and K_2CO_3 (1.07 g) was refluxed in acetone (100 mL) for 20 hours. The suspension was hot filtered and the solvent was removed under reduced pressure. After adding petroleum ether, the residue was kept at -18 °C overnight and the yellow solid that formed was filtered off, affording **16** (1.12 g, 85 %). mp $97-98$ °C. ^1H NMR δ : 1.10 (t, 3H, $J = 6.4$ Hz), 1.93-2.08 (m, 4H), 2.56 (q, 2H, $J = 6.4$ Hz), 3.60-3.75 (m, 6H), 4.05 (t, 2H, $J = 6.2$ Hz), 6.95 (d, 1H, Ar), 7.15 (dd, 1H, Ar), 7.20-7.55 (m, 8H, Ar), 7.65 (d, 2H, $J = 8.8$ Hz, Ar), 7.75 (s, 1H, Ar). ^{13}C NMR δ : 12.06, 24.02, 27.86, 45.71, 47.34, 57.57 (2C), 68.74, 110.83, 113.85, 117.66, 122.75, 124.84, 126.92, 128.30, 128.49, 128.66, 128.85, 133.37, 134.41, 137.88, 139.47, 141.25, 147.98, 160.58.

This item was downloaded from IRIS Università di Bologna (<https://cris.unibo.it/>)

When citing, please refer to the published version.

3-(4-((benzyl(ethyl)amino)methyl)phenyl)-6-(5-chloropentyloxy)-2H-chromen-2-one (17).

Using the previous procedure and starting from **14** (0.98 g, 2.55 mmol) and 1-bromo-5-chloropentane (0.67 mL, 5.1 mmol), **17** was obtained as a yellow solid (1.0 g, 80 %). mp 97-98 °C. ¹H NMR δ: 1.12 (t, 3H, *J* = 6.4 Hz), 1.60-1.75 (m, 2H), 1.80-2.00 (m, 4H), 2.50 (q, 2H, *J* = 6.4 Hz), 3.55-3.65 (m, 6H), 4.03 (t, 2H, *J* = 6.2 Hz), 6.97 (d, 1H, Ar), 7.17 (dd, 1H, Ar), 7.20-7.55 (m, 8H, Ar), 7.63 (d, 2H, *J* = 8.8 Hz, Ar), 7.70 (s, 1H, Ar). ¹³C NMR δ: 11.86, 23.92, 27.36, 29.88, 47.13, 52.80 (2C), 57.74, 68.61, 110.57, 117.34, 122.83, 124.78, 126.73, 128.14, 128.36, 128.51, 128.68, 128.79, 133.20, 139.31, 139.87, 140.76, 141.09, 147.81, 160.82.

3-(4-((benzyl(ethyl)amino)methyl)phenyl)-7-(4-chlorobutoxy)-2H-chromen-2-one (18). Using the previous procedure and starting from **15** (0.55 g, 1.43 mmol) and 1-bromo-4-chlorobutane (0.33 mL, 2.86 mmol), **18** was obtained as a yellow solid (0.68 g, 98 %). mp 98-99 °C. ¹H NMR δ: 1.13 (t, 3H, *J* = 5.7 Hz), 1.95-2.05 (m, 4H), 2.51 (q, 2H, *J* = 5.7 Hz), 3.55-3.65 (m, 6H), 4.05 (t, 2H, *J* = 6.2 Hz), 6.93 (d, 2H, Ar), 7.25-7.45 (m, 8H, Ar), 7.62 (d, 2H, *J* = 8.8 Hz, Ar), 7.80 (s, 1H, Ar). ¹³C NMR δ: 12.09, 24.23, 27.87, 45.73, 47.34, 57.58 (2C), 68.74, 110.87, 113.84, 117.86, 122.77, 124.91, 126.96, 128.33, 128.49, 128.68, 128.85, 133.56, 134.44, 137.86, 139.48, 141.25, 147.88, 160.55.

3-(4-((benzyl(ethyl)amino)methyl)phenyl)-7-((5-chloropentyl)oxy)-2H-chromen-2-one (19).

Using the previous procedure and starting from **15** (0.75 g, 1.95 mmol) and 1-bromo-5-chloropentane (0.55 mL, 3.9 mmol), **19** was obtained as a yellow solid (0.75 g, 79 %). mp 30-31 °C. ¹H NMR δ: 1.10 (t, 3H, *J* = 5.8 Hz), 1.55-1.65 (m, 2H), 1.75-1.95 (m, 4H), 2.58 (q, 2H, *J* = 5.8 Hz), 3.56-3.62 (m, 6H), 4.05 (t, 2H, *J* = 6.2 Hz), 6.78-6.85 (m, 2H, Ar), 7.15-7.43 (m, 8H, Ar), 7.63 (d, 2H, *J* = 8.8 Hz, Ar), 7.70 (s, 1H, Ar). ¹³C NMR δ: 12.01, 24.33, 27.88, 45.74, 47.38, 57.58 (2C), 68.83, 110.84, 113.76, 117.86, 122.88, 124.82, 127.02, 128.32, 128.49, 128.65, 128.89, 133.41, 134.49, 137.88, 139.57, 141.27, 147.93, 160.58.

This item was downloaded from IRIS Università di Bologna (<https://cris.unibo.it/>)

When citing, please refer to the published version.

3-(4-((benzyl(ethyl)amino)methyl)phenyl)-6-(4-iodobutoxy)-2H-chromen-2-one (20). A mixture of **16** (0.17 g, 0.36 mmol) and NaI (46 mg, 0.36 mmol) in methylethylketone (40 mL) was refluxed for 4 h, then the solvent was concentrated under reduced pressure. The crude was dissolved in DCM and washed with water. The organic layer was collected, dried over Na₂SO₄ and the solvent was evaporated under reduced pressure, affording **20** as a yellow solid (0.13 g), that was used for the next reaction without any further purification.

3-(4-((benzyl(ethyl)amino)methyl)phenyl)-6-((5-iodopentyl)oxy)-2H-chromen-2-one (21). Using the previous procedure and starting from **17** (0.27 g, 0.55 mmol), **21** was obtained as a yellow solid (0.3 g).

3-(4-((benzyl(ethyl)amino)methyl)phenyl)-7-(4-iodobutoxy)-2H-chromen-2-one (22). Using the previous procedure and starting from **18** (0.6 g, 1.26 mmol), **22** was obtained as a yellow solid (0.43 g).

3-(4-((benzyl(ethyl)amino)methyl)phenyl)-7-((5-iodopentyl)oxy)-2H-chromen-2-one (23). Using the previous procedure and starting from **19** (0.75 g, 1.5 mmol), **23** was obtained as a yellow oil (0.5 g).

General procedure for the synthesis of compounds 3-11.

By using a parallel procedure, in distinct reactors the selected iododerivatives (**20-23**, 0.5 mmol) were dissolved in toluene (20 mL), then the selected amine (0.5 mmol) and Et₃N (0.5 mmol) were added. The reaction mixtures were stirred under reflux for 20 h while monitoring with TLC, then they were washed with water (3 x 25 mL) and the organic layers were dried over Na₂SO₄. The solvent was removed under reduced pressure and the residue was purified by flash chromatography (toluene/acetone 3:2).

3-(4-((benzyl(ethyl)amino)methyl)phenyl)-6-(4-(diethylamino)butoxy)-2H-chromen-2-one (3). Yellow solid mp 111-112 °C (ligroin). ¹H NMR δ: 1.05-1.15 (m, 9H), 1.63-1.70 (m, 2H), 1.77-1.85

This item was downloaded from IRIS Università di Bologna (<https://cris.unibo.it/>)

When citing, please refer to the published version.

(m, 2H), 2.55-2.60 (m, 8H), 3.57 (s, 4H), 4.01 (t, 2H, $J = 6.2$ Hz), 6.97 (d, 1H, Ar), 7.15 (dd, 1H, Ar), 7.20-7.50 (m, 8H, Ar), 7.63 (d, 2H, $J = 8.8$ Hz, Ar), 7.75 (s, 1H, Ar). ^{13}C NMR δ : 11.86 (2C), 12.05, 23.82, 27.44, 47.01 (2C), 47.30, 52.71, 57.57, 57.91, 68.74, 110.77, 113.82, 117.51, 119.63, 120.22, 122.75, 124.83, 126.90, 128.30, 128.49, 128.66, 128.85, 133.37, 137.88, 139.47 (2C), 140.04, 141.25, 147.98, 155.75, 160.98. MS (ES) m/z : 513 (M+1). Calcd for $\text{C}_{33}\text{H}_{40}\text{N}_2\text{O}_3$: C 77.31, H 7.86, N 5.46, found: C $\langle \rangle \langle \rangle \langle \rangle$, H $\langle \rangle \langle \rangle \langle \rangle$, N

3-(4-((benzyl(ethyl)amino)methyl)phenyl)-6-((5-(diethylamino)pentyl)oxy)-2H-chromen-2-one

(4). Yellow solid mp 90-91 °C (ligroin). ^1H NMR δ : 1.03-1.17 (m, 9H), 1.45-1.60 (m, 4H), 1.80-1.90 (m, 2H), 2.43-2.61 (m, 8H), 3.61 (s, 4H), 4.01 (t, 2H, $J = 6.2$ Hz), 6.92 (d, 1H, Ar), 7.13 (dd, 1H, Ar), 7.17-7.45 (m, 8H, Ar), 7.61 (d, 2H, $J = 8.8$ Hz, Ar), 7.73 (s, 1H, Ar). ^{13}C NMR δ : 11.62 (2C), 11.89, 24.12, 26.86, 29.16, 46.87 (2C), 47.13, 52.80, 57.40, 57.74, 68.61, 110.57, 117.34, 119.45, 120.05, 121.32, 122.83, 124.78, 126.73, 128.14, 128.33, 128.49, 128.68, 133.20, 139.31 (2C), 139.87, 140.76, 141.09, 147.81, 155.60, 160.82. MS (ES) m/z : 527 (M+1). Calcd for $\text{C}_{34}\text{H}_{42}\text{N}_2\text{O}_3$: C 77.53, H 8.04, N 5.32, found: C $\langle \rangle \langle \rangle \langle \rangle$, H $\langle \rangle \langle \rangle \langle \rangle$, N

3-(4-((benzyl(ethyl)amino)methyl)phenyl)-6-((5-morpholinopentyl)oxy)-2H-chromen-2-one

(5). Yellow solid mp 82-83 °C (ligroin). ^1H NMR δ : 1.10 (t, 3H, $J = 6.6$ Hz), 1.40-1.65 (m, 4H), 1.77-1.90 (m, 2H), 2.25-2.60 (m, 8H), 3.57 (s, 4H), 3.70 (m, 4H), 3.97 (t, 2H, $J = 6.2$ Hz), 6.97 (d, 1H, Ar), 7.13 (dd, 1H, Ar), 7.17-7.45 (m, 8H, Ar), 7.63 (d, 2H, $J = 8.8$ Hz, Ar), 7.78 (s, 1H, Ar). ^{13}C NMR δ : 11.98, 24.33, 25.74 (2C), 26.69, 29.31, 47.33, 54.78, 57.57, 58.02, 59.44 (2C), 68.72, 110.68, 113.22, 117.52, 119.68, 120.15, 122.87, 127.03, 128.41, 128.53, 128.68, 128.83, 133.48 (2C), 138.08, 138.52, 139.48, 140.15, 141.28, 147.99, 155.56, 160.88. MS (ES) m/z : 541 (M+1). Calcd for $\text{C}_{34}\text{H}_{40}\text{N}_2\text{O}_4$: C 75.53, H 7.46, N 5.18, found: C $\langle \rangle \langle \rangle \langle \rangle$, H $\langle \rangle \langle \rangle \langle \rangle$, N

3-(4-((benzyl(ethyl)amino)methyl)phenyl)-6-((5-(piperidin-1-yl)pentyl)oxy)-2H-chromen-2-

one (6). White solid mp 105-106 °C (ligroin). ^1H NMR δ : 1.13 (t, 3H, $J = 6.3$ Hz), 1.40-1.64 (m,

This item was downloaded from IRIS Università di Bologna (<https://cris.unibo.it/>)

When citing, please refer to the published version.

10H), 1.78-1.85 (m, 2H), 2.30-2.45 (m, 6H), 2.58 (q, 2H, $J = 6.3$ Hz), 3.58 (s, 4H), 4.00 (t, 2H, $J = 6.2$ Hz), 6.97 (d, 1H, Ar), 7.10 (dd, 1H, Ar), 7.23-7.52 (m, 8H, Ar), 7.63 (d, 2H, $J = 8.8$ Hz, Ar), 7.78 (s, 1H, Ar). ^{13}C NMR δ : 12.05, 24.30, 24.52, 25.98 (2C), 26.70, 29.26, 47.31, 54.73, 57.57, 57.92, 59.41 (2C), 68.69, 110.75, 113.00, 117.52, 119.61, 120.22, 122.81, 126.89, 128.30, 128.49, 128.67, 128.86, 133.38 (2C), 137.98, 138.52, 139.46, 140.05, 141.25, 147.99, 155.76, 160.98. MS (ES) m/z : 539 (M+1). Calcd for $\text{C}_{35}\text{H}_{42}\text{N}_2\text{O}_3$: C 78.03, H 7.86, N 5.20, found: C $\langle \rangle \langle \rangle$, H $\langle \rangle \langle \rangle$, N

3-(4-((benzyl(ethyl)amino)methyl)phenyl)-6-((5-(4-phenylpiperazin-1-yl)pentyl)oxy)-2H-chromen-2-one (7). White solid mp 87-89 °C (ligroin). ^1H NMR δ : 1.12 (t, 3H, $J = 6.6$ Hz), 1.55-1.70 (m, 4H), 1.75-1.93 (m, 2H), 2.40-2.70 (m, 8H), 3.21-3.32 (m, 4H), 3.62 (s, 4H), 4.01 (t, 2H, $J = 6.2$ Hz), 6.80-6.97 (m, 4H, Ar), 7.12 (dd, 1H, Ar), 7.15-7.47 (m, 10H, Ar), 7.60-7.75 (m, 3H, Ar). ^{13}C NMR δ : 11.88, 24.05, 26.61, 29.11, 47.14, 49.11 (2C), 53.30, 57.40, 57.74, 58.52 (2C), 68.51, 110.59, 114.03, 114.88, 115.99, 117.37, 119.41, 119.66, 120.07, 126.72, 126.74, 127.23, 128.14, 128.33, 128.53, 128.69, 129.08, 133.20, 139.27, 139.87, 141.10, 143.38, 147.83, 148.02, 151.29, 155.57, 160.79. MS (ES) m/z : 616 (M+1). Calcd for $\text{C}_{40}\text{H}_{45}\text{N}_3\text{O}_3$: C 78.02, H 7.37, N 6.82, found: C $\langle \rangle \langle \rangle \langle \rangle$ 78.07, H $\langle \rangle \langle \rangle \langle \rangle$, N

3-(4-((benzyl(ethyl)amino)methyl)phenyl)-6-((5-(4-phenylpiperidin-1-yl)pentyl)oxy)-2H-chromen-2-one (8). White solid mp 86-87 °C (ligroin). ^1H NMR δ : 1.10 (t, 3H, $J = 6.6$ Hz), 1.43-1.63 (m, 4H), 1.75-1.86 (m, 5H), 1.98-2.11 (m, 2H), 2.34-2.61 (m, 6H), 3.05-3.18 (m, 2H), 3.58 (s, 4H), 4.00 (t, 2H, $J = 6.2$ Hz), 6.93 (d, 1H, $J = 1.9$ Hz, Ar), 7.13-7.53 (m, 14H, Ar), 7.61 (d, 2H, $J = 8.1$ Hz, Ar), 7.73 (s, 1H, Ar). ^{13}C NMR δ : 11.89, 24.15, 26.77, 29.12, 33.40 (2C), 42.72, 47.14, 54.42, 57.40, 57.74, 58.92 (2C), 68.52, 110.58, 113.33, 117.36, 119.21, 119.44, 120.07, 126.12, 126.74, 126.83, 127.01, 128.14, 128.33, 128.39, 128.51, 128.69, 133.20, 133.77, 134.35, 137.82, 139.30, 139.87, 141.09, 146.30, 147.82, 155.59, 160.81. MS (ES) m/z : 615 (M+1). Calcd for $\text{C}_{41}\text{H}_{46}\text{N}_2\text{O}_3$: C 80.10, H 7.54, N 4.56, found: C $\langle \rangle \langle \rangle \langle \rangle$ 78.07, H $\langle \rangle \langle \rangle \langle \rangle$, N

This item was downloaded from IRIS Università di Bologna (<https://cris.unibo.it/>)

When citing, please refer to the published version.

3-(4-((benzyl(ethyl)amino)methyl)phenyl)-6-((5-(3,4-dihydroisoquinolin-2(1H)-yl)pentyl)oxy)-2H-chromen-2-one (9). Yellow solid mp 93-94 °C (ligroin). ¹H NMR δ: 1.11 (t, 3H, *J* = 6.6 Hz), 1.57-1.77 (m, 4H), 1.84-1.93 (m, 2H), 2.50-2.60 (m, 4H), 2.77 (t, 2H, *J* = 5.8 Hz), 2.97 (t, 2H, *J* = 6.2 Hz), 3.58-3.65 (m, 4H), 4.00 (t, 2H, *J* = 6.2 Hz), 6.97 (d, 1H, *J* = 1.9 Hz, Ar), 7.08-7.20 (m, 4H, Ar), 7.23-7.47 (m, 10H, Ar), 7.62 (d, 2H, *J* = 8.4 Hz, Ar), 7.78 (s, 1H, Ar). ¹³C NMR δ: 11.88, 24.02, 26.81, 28.88, 29.10, 47.13, 56.03, 57.39, 57.73, 58.06 (2C), 68.54, 110.59, 113.38, 117.36, 119.45, 120.06, 122.64, 124.16, 125.62, 125.88, 126.15, 126.57, 126.75, 127.42, 127.48, 128.15, 128.33, 128.50, 128.63, 128.70, 133.21, 134.18, 139.32, 139.85, 141.06, 147.82, 155.58, 160.83. MS (ES) *m/z*: 587 (M+1). Calcd for C₃₉H₄₂N₂O₃: C 79.83, H 7.22, N 4.77, found: C 79.83, H 7.22, N 4.77.

3-(4-((benzyl(ethyl)amino)methyl)phenyl)-7-(4-(diethylamino)butoxy)-2H-chromen-2-one (10). Yellow solid mp 50-51 °C (ligroin). ¹H NMR δ: 1.03-1.15 (m, 9H), 1.60-1.75 (m, 2H), 1.77-1.91 (m, 2H), 2.40-2.60 (m, 8H), 3.56 (s, 4H), 4.10 (t, 2H, *J* = 6.2 Hz), 6.82-6.89 (m, 2H, Ar), 7.22-7.43 (m, 8H, Ar), 7.63 (d, 2H, *J* = 8.4 Hz, Ar), 7.76 (s, 1H, Ar). ¹³C NMR δ: 11.75 (2C), 12.02, 23.63, 27.20, 46.92 (2C), 47.24, 52.56, 57.54, 57.86, 68.60, 101.00, 111.06, 113.24, 113.40, 117.72, 122.83, 124.70, 126.85, 128.27, 128.28, 128.81, 128.82, 133.60, 134.18, 137.84, 139.81 (2C), 140.04, 140.68, 155.34, 161.14. MS (ES) *m/z*: 513 (M+1). Calcd for C₃₃H₄₀N₂O₃: C 77.31, H 7.86, N 5.46, found: C 77.31, H 7.86, N 5.46.

3-(4-((benzyl(ethyl)amino)methyl)phenyl)-7-((5-(diethylamino)pentyl)oxy)-2H-chromen-2-one (11). Yellow solid mp 64-65 °C (ligroin). ¹H NMR δ: 1.05-1.17 (m, 9H), 1.40-1.63 (m, 4H), 1.78-1.90 (m, 2H), 2.45-2.65 (m, 8H), 3.61 (s, 4H), 4.02 (t, 2H, *J* = 6.2 Hz), 6.81-6.85 (m, 2H, Ar), 7.15-7.47 (m, 8H, Ar), 7.63 (d, 2H, *J* = 8.8 Hz, Ar), 7.77 (s, 1H, Ar). ¹³C NMR δ: 11.68 (2C), 11.92, 24.13, 26.27, 29.25, 46.92 (2C), 47.14, 52.86, 57.54, 57.86, 68.60, 110.88, 117.24, 119.40, 120.18, 121.56, 122.91, 124.70, 126.85, 127.18, 127.71, 128.27, 128.28, 128.69, 128.82, 133.64, 139.81 (2C), 139.94,

140.04, 140.68, 155.64, 161.03. MS (ES) m/z : 527 (M+1). Calcd for $C_{34}H_{42}N_2O_3$: C 77.53, H 8.04, N 5.32, found: C 77.53, H 8.04, N 5.32.

10-chloro-1-methoxy-11*H*-indeno[1,2-*b*]quinoline (25). To a mixture of 2-aminobenzoic acid (0.21 g, 1.5 mmol) and 4-methoxy-2,3-dihydro-1*H*-inden-1-one (0.25 g, 1.5 mmol), POCl₃ (10 mL) was carefully added. The mixture was heated under reflux for 2 h, then poured into ice. The mixture was basified with NaHCO₃ and filtered, affording **25** which was purified by flash chromatography (DCM), (0.20 g, 46 %), mp 198-199 °C. ¹H NMR δ: 3.54 (s, 2H), 3.85 (s, 3H), 6.97 (d, 1H, J = 7.6 Hz, Ar), 7.34 (s, 1H, Ar), 7.47-7.86 (m, 4H, Ar), 8.17-8.31 (m, 1H, Ar). ¹³C NMR δ: 24.99, 55.58, 110.68, 114.72, 122.13, 123.94, 124.34, 126.24, 128.14, 129.54, 132.17, 139.21, 141.85, 141.12, 146.43, 155.16, 155.39.

6-(5-aminopentyl)-3-(4-((benzyl(ethyl)amino)methyl)phenyl)-2*H*-chromen-2-one (26). A suspension of **17** (0.7 g, 14.7 mmol) and potassium phthalimide salt (2.7 g, 14.7 mmol) in DMF (10 mL) was refluxed for 2 hours. The reaction mixture was poured into ice/water and the formed precipitate was filtered under vacuum (0.75 g, 85 %). A stirred solution of this intermediate (0.59 g, 0.98 mmol) and hydrazine monohydrate (0.1 mL, 3.05 mmol) in EtOH (10 mL) was refluxed for 4 hours. Conc. HCl (0.3 mL) was then added portionwise and the mixture was allowed to reflux for 30 minutes. The solvent was removed and the residue was treated with water and made alkaline by K₂CO₃. The aqueous phase was extracted with DCM, which was then dried over Na₂SO₄ and evaporated affording **26** as an oil, which was purified by flash chromatography (toluene/acetone 4:1), (0.31 g, 52 %). ¹H NMR δ: 1.07 (t, 3H, J = 6.4 Hz), 1.45-1.51 (m, 4H), 1.79-1.88 (m, 2H), 2.50-2.60 (m, 2H), 2.63-2.72 (m, 2H), 3.58 (s, 4H), 3.98 (t, 2H, J = 6.2 Hz), 6.93 (s, 1H, Ar), 7.08 (d, 1H, J = 2.4 Hz, Ar), 7.20-7.45 (m, 8H, Ar), 7.62 (d, 2H, J = 8.0 Hz, Ar), 7.72 (s, 1H, Ar). ¹³C NMR δ: 12.37, 27.10, 29.96, 32.45, 36.92, 41.25, 48.79, 58.08 (2C), 116.72, 120.97, 126.56,

This item was downloaded from IRIS Università di Bologna (<https://cris.unibo.it/>)

When citing, please refer to the published version.

126.73, 127.18, 127.88, 127.97, 128.48, 128.95, 131.50, 133.17, 138.23, 138.36, 141.98, 145.36, 154.16, 161.03.

3-(4-((benzyl(ethyl)amino)methyl)phenyl)-6-(2-((7-methoxy-6*H*-indeno[2,1-*b*]quinolin-11-yl)amino)ethoxy)-2*H*-chromen-2-one (12). A stirred suspension of **25** (0.1 g, 0.36 mmol) and phenol (15 mL) was heated at 85-90 °C until a solution was obtained. Then, **24**^[17] (0.15 g, 0.36 mmol) was added and the reaction mixture was heated to 130 °C for 4 hours. The crude was extracted with ethyl acetate (3 x 20 mL) and the collected organic layers were washed with NaOH 2N solution, dried over Na₂SO₄ and evaporated to dryness. The residue was purified by flash chromatography (DCM/methanol 98:2). ¹H NMR δ: 1.08 (t, 3H, *J* = 6.6 Hz), 2.52 (q, 2H, *J* = 6.6 Hz), 3.60 (s, 4H), 3.83 (s, 2H), 3.94 (s, 3H), 4.06-4.28 (m, 4H), 6.95 (d, 1H, Ar), 7.25-7.67 (m, 16H, Ar), 7.81-7.94 (m, 2H, Ar), 8.16 (s, 1H, Ar). ¹³C NMR δ: 11.84, 29.38, 47.51, 53.45, 55.58, 57.42, 57.55, 68.28, 110.15, 110.82, 113.77, 117.33, 117.56, 119.28, 120.24, 122.11, 122.77, 124.04, 126.75, 126.88, 128.15, 128.36, 128.51, 128.58, 128.68, 128.83, 129.54, 133.17, 134.01, 139.22, 139.63, 139.88, 140.02, 141.05, 141.18, 142.67, 142.78, 146.55, 147.52, 147.91, 155.49, 161.03. The product was then converted in the hydrochloride salt affording **12 HCl** mp 230-232 °C (MeOH). MS (ES) *m/z*: 674 (M+1). Calcd for C₄₄H₄₀ClN₃O₄: C 77.41, H 5.68, N 5.92, found: C <?>?<?>7, H <?>?<?>, N

3-(4-((benzyl(ethyl)amino)methyl)phenyl)-6-((5-((7-methoxy-6*H*-indeno[2,1-*b*]quinolin-11-yl)amino)pentyl)oxy)-2*H*-chromen-2-one (13). A stirred suspension of **25** (0.07 g, 0.25 mmol), **26** (0.12 g, 0.25 mmol) and 1-pentanol (0.3 mL) was heated at 180 °C for 18 h, then cooled to room temperature. DCM was added (20 mL) and the organic layer was washed with NaOH 10% aqueous solution, dried over Na₂SO₄ and evaporated to dryness. The residue was purified by flash chromatography (toluene/acetone 4:1) affording **13** as dark yellow oil. ¹H NMR δ: 1.08 (t, 3H, *J* = 6.6 Hz), 1.71-1.73 (m, 2H), 1.82-1.92 (m, 4H), 2.35-2.40 (m, 2H), 2.52 (q, 2H, *J* = 6.6 Hz), 3.60 (s,

This item was downloaded from IRIS Università di Bologna (<https://cris.unibo.it/>)

When citing, please refer to the published version.

4H), 3.79-3.80 (m, 2H), 3.88 (s, 3H), 4.01 (t, 2H, $J = 6.2$ Hz), 4.83 (broad, 1H, NH), 6.88 (s, 1H, Ar), 7.01-7.76 (m, 17H, Ar), 8.02 (d, 1H, $J = 8.8$ Hz, Ar), 8.14 (s, 1H, Ar). ^{13}C NMR δ : 11.87, 23.39, 29.33, 29.67, 31.89, 47.13, 53.40, 55.50, 57.39, 57.73, 68.24, 109.85, 110.60, 113.72, 117.36, 117.48, 119.26, 120.08, 122.13, 122.86, 123.94, 126.74, 126.78, 128.14, 128.33, 128.49, 128.52, 128.69, 128.75, 129.54, 133.14, 133.99, 139.21, 139.63, 139.84, 139.84, 141.05, 141.12, 142.66, 142.78, 146.43, 147.49, 147.85, 155.39, 161.45. MS (ES) m/z : 716 ($M+1$). Calcd for $\text{C}_{47}\text{H}_{45}\text{N}_3\text{O}_4$: C 78.85, H 6.34, N 5.87, found: C 78.85, H 6.34, N 5.87.

Biological assay

Human AChE and BuChE Inhibition Assay. AChE inhibitory activity was evaluated spectrophotometrically at 37 °C by Ellman's method^[18] using a Jasco V-530 double beam spectrophotometer. The rate of increase in the absorbance at 412 nm was followed for 5 min. AChE stock solution was prepared by dissolving human recombinant AChE (E.C.3.1.1.7) lyophilized powder (Sigma, Italy) in 0.1 M phosphate buffer (pH = 8.0) containing Triton X-100 0.1 %. Stock solution of BuChE (E.C. 3.1.1.8) from human serum (Sigma, Italy) was prepared by dissolving the lyophilized powder in an aqueous solution of gelatine 0.1 %. Stock solutions of inhibitors (1 or 2 mM) were prepared in methanol. The assay solution consisted of a 0.1 M phosphate buffer pH 8.0, with the addition of 340 μM 5,5'-dithiobis(2-nitrobenzoic acid), 0.02 unit/mL human recombinant AChE or human serum BuChE, and 550 μM substrate (acetylthiocholine iodide or butyrylthiocholine iodide, respectively). 50 μL aliquots of increasing concentration of the tested compound were added to the assay solution and preincubated for 20 min at 37 °C with the enzyme followed by the addition of substrate. Assays were carried out with a blank containing all

This item was downloaded from IRIS Università di Bologna (<https://cris.unibo.it/>)

When citing, please refer to the published version.

components except AChE or BuChE in order to account for the non-enzymatic reaction. The reaction rates were compared and the percent inhibition due to the presence of tested inhibitor at increasing concentration was calculated. At least two independent experiments were carried out. In each experiment, each inhibitor concentration was analyzed in duplicate, and the IC₅₀ values were determined graphically from log concentration–inhibition curves (GraphPad Prism 4.03 software, GraphPad Software Inc.).

Inhibition of A β ₄₂ self-aggregation. As reported in a previously published protocol,^[30] HFIP pretreated A β ₄₂ samples (Bachem AG, Switzerland) were solubilized with a CH₃CN/0.3 mM Na₂CO₃/250 mM NaOH (48.4:48.4:3.2) mixture. Experiments were performed by incubating the peptide in 10 mM phosphate buffer (pH = 8.0) containing 10 mM NaCl, at 30 °C for 24 h (final A β concentration = 50 μ M) with and without inhibitor (50 μ M, A β /inhibitor = 1/1). Blanks containing the tested inhibitors were also prepared and tested. To quantify amyloid fibrils formation, the thioflavin T fluorescence method was used.^[24] After incubation, samples were diluted to a final volume of 2.0 mL with 50 mM glycine–NaOH buffer (pH 8.5) containing 1.5 μ M thioflavin T. A 300-second-time scan of fluorescence intensity was carried out (λ_{exc} = 446 nm; λ_{em} = 490 nm, FP-6200 fluorometer, Jasco Europe), and values at plateau were averaged after subtracting the background fluorescence of 1.5 μ M thioflavin T solution. The fluorescence intensities were compared and the percent inhibition due to the presence of the inhibitor was calculated by the following formula: $100 - (IF_i/IF_o \times 100)$ where IF_i and IF_o are the fluorescence intensities obtained for A β ₄₂ in the presence and in the absence of inhibitor, respectively.

This item was downloaded from IRIS Università di Bologna (<https://cris.unibo.it/>)

When citing, please refer to the published version.

Cell cultures

Human neuronal (SH-SY5Y) cells were routinely grown in Dulbecco's modified Eagle' Medium (DMEM) supplemented with 10% fetal bovine serum, 2 mmol/L glutamine, 50 U mL⁻¹ penicillin and 50 µg mL⁻¹ streptomycin at 37°C in a humidified incubator with 5% CO₂.

Determination of acute neurotoxicity of compounds

To evaluate the acute neurotoxicity of compounds **2**, **4-7**, **9**, **10** and **12**, the SH-SY5Y cells were seeded in 96-well plates at 2×10^4 cells/well, incubated for 24 h and subsequently treated with various concentrations [1.25 - 40 µM] of compounds for 4 h at 37° C in 5% CO₂.

The cell viability in terms of mitochondrial metabolic function was evaluated by the reduction in 3-(4,5-dimethyl-2-thiazolyl)-2,5-diphenyl-2H-tetrazolium bromide (MTT) to formazan as previously described (reference 23). The quantity of formazan was directly proportional to the number of viable cells. Briefly, the treatment medium was replaced with MTT (5 mg/mL) in phosphate-buffered saline (PBS) for 2 h at 37°C in 5% CO₂. After washing with PBS, the formazan crystals were dissolved with isopropanol. The amount of formazan was measured (570 nm, ref. 690 nm) using a Multilabel Plate Reader (VICTOR™ X3, PerkinElmer, Massachusetts, USA). The neurotoxicity is expressed as a percentage of control cells.

Aβ₄₂ oligomers preparation

Aβ₄₂ peptide (Diatech Pharmacogenetics srl, Jesi, Italy) was first dissolved in hexafluoroisopropanol to 1 mg mL⁻¹, sonicated, incubated at room temperature for 24 h and lyophilized. The resulting unaggregated Aβ₄₂ peptide film was dissolved with dimethylsulfoxide [1 mM] and stored at -20°C

This item was downloaded from IRIS Università di Bologna (<https://cris.unibo.it/>)

When citing, please refer to the published version.

until use. The A β ₄₂ aggregation to oligomeric form was prepared in serum-free DMEM [40 μ M] and stored at 4°C for 24 h.^[31]

Determination of A β ₄₂ oligomer-induced cytotoxicity

To evaluate the protective effects of compounds against A β ₄₂ oligomer- induced cytotoxicity, the SH-SY5Y cells were seeded in 96-well plates at 2×10^4 cells/well, incubated for 24 h and subsequently treated with A β ₄₂ oligomers [10 μ M] for 4 h at 37°C in 5% CO₂, in the presence of compounds **4** and **10** [1 μ M]. The cell viability was evaluated by MTT assay as described in “Determination of acute neurotoxicity of compounds” subsection.^[31] The neurotoxicity is expressed as a percentage of control cells.

Modelling on hAChE

Ligand Preparation

Ligands were prepared with the LigPrep tool available in the Schrödinger Suite 2014-3. Ionization states were generated at pH 7.0 ± 2.0 with Epik.

Protein Preparation

The X-ray coordinates of Recombinant Human Acetylcholinesterase in complex with Donepezil were extracted from the Protein Data Bank (PDB code 4EY7). The structure was then processed with the Schrödinger Suite 2014-3 Protein Preparation Wizard tool. The B Chain was deleted, water molecules were removed, and an exhaustive sampling of the orientations of groups, whose hydrogen bonding network needs to be optimized, was performed. Finally, the protein structure was

This item was downloaded from IRIS Università di Bologna (<https://cris.unibo.it/>)

When citing, please refer to the published version.

refined to relieve steric clashes with a restrained minimization with the OPLS2005 force field until a final rmsd of 0.30 Å with respect to the input protein coordinates.

Docking

Docking studies were performed using Glide V65013. The protein structure, prepared as described above, was used to build the energy grid. The enclosing box was centered on the cocrystallized ligand. A size of 10 Å and 40 Å was used for the INNERBOX and OUTERBOX, respectively.

The SP docking protocol with an enhanced sampling of 2 and the canonicalize input conformation option was used. All other parameters were set to their default value.

The docking protocol was validated by redocking the cocrystallized ligand Donepezil.

Five different poses were saved, sorted by GlideScore and, finally, visually inspected.

Molecular Dynamics

A molecular dynamics of the complexes resulting from docking of both **4** and **7** was performed using Desmond v40013.

Each complex was neutralized using sodium counter ions. The complexes and the counter ions were immersed in a orthorhombic periodic SPC water bath that extended about 10 Å in each direction.

After an initial default relaxation protocol, an MD production run was performed for 24.0 ns with a time step of 2.0 ps.

Modelling on A β ₄₂

This item was downloaded from IRIS Università di Bologna (<https://cris.unibo.it/>)

When citing, please refer to the published version.

The ligand structures were built by using the Schrödinger Software (v.2.1, Maestro 9.5.0.14) and minimized by semi-empirical NDDO Module PM3. The force field parameters of ligands were obtained using ParamChem server employing CGenFF (CHARMM General Force Field) for small molecules.^[32] The structure of A β ₄₂ in oligomeric fibril form, involving five monomers, was taken from NMR structure from Protein Data Bank (PDB id:2BEG).^[33] Since only part of the structure is visible (residues 17-42) the lacking residues were added by incorporating 16-residue fragment from NMR structure of A β ₁₋₂₈ (PDB id:1BJC).^[34] The fragment 1-16 exists in the coil form. Different NMR conformations of this 1-16 fragment were selected for each monomer of the fibril. Two identical ligands were inserted at both ends of the fibril, one at each side, in a distance 2.5 Å on average. All energy minimizations and molecular dynamics (MD) simulations were performed in NAMD program version 2.10 using all-atom force field CHARMM22^[35] in implicit solvent. All figures of molecular structures were created using VMD program (v.1.9.2).^[36]

The simulated systems were initially subjected to 10 000 steps of energy minimization and then 100 ns MD equilibration with increasing temperature from 20 K to 298 K. The MD simulations were conducted using Langevin (stochastic) dynamics^[37] which is default in the NAMD program. The molecules in the system interact with a stochastic heat bath via random forces and dissipative forces. The friction coefficient of 50 ps⁻¹ was used and temperature was set to 298 K. Non-bonded interactions were damped employing a switching function for van der Waals and electrostatic interactions using cutoff of 14 Å. For each investigated system 600 ns MD simulation was performed with a time step of 2 fs. All bond lengths were constrained using SHAKE algorithm.^[38]

Acknowledgements. This work was supported by the University of Bologna and by the Italian Ministry for Education, Universities and Research (MIUR). VA also thank Unirimini for financial support.

References

- [1] C. Ballard, S. Gauthier, A. Corbett, C. Brayne, D. Aarsland, E. Jones, *The Lancet* **2011**, 9770, 1019-1031.
- [2] A. Contestabile, *Behav. Brain Res.* **2011**, 221, 334-340.
- [3] L. A. Craig, N. S. Hong, R. J. McDonald, *Neurosci. Biobehav. R.* **2011**, 35, 1397–1409.
- [4] B. Reisberg, R. Doody, A. Stöffler, F. Schmitt, S. Ferris, H. J. Möbius, *N. Engl. J. Med.* **2003**, 348, 1333-1341.
- [5] C. L. Masters, D. J. Selkoe, *Cold Spring Harb. Perspect. Med.* **2012**, 2:a006262.
- [6] J. Avila, *FEBS Lett.* **2006**, 580, 2922-2927.
- [7] D.J. Selkoe, *Behav. Brain Res.* **2008**, 192, 106-113.
- [8] J. Hardy, D. J. Selkoe, *Science* **2002**, 297, 353–356.
- [9] S. T. Ferreira, M. V. Lourenco, M. M. Oliveira, F. G. De Felice, *Front. Cell. Neurosci.* **2015**, 9, 191.
- [10] H. Fukumoto, T. Tokuda, T. Kasai, N. Ishigami, H. Hidaka, M. Kondo, D. Allsop, M. Nakagawa, *FASEB J.*, **2010**, 24, 2716–2726.

This item was downloaded from IRIS Università di Bologna (<https://cris.unibo.it/>)

When citing, please refer to the published version.

- [11] Y. Gong, L. Chang, K. L. Viola, P. N. Lacor, M. P. Lambert, C. E. Finch, G. A. Krafft, W. L. Klein, *Proc. Natl. Acad. Sci. U S A* **2003**, *100*, 10417–10422.
- [12] R. Morphy, Z. Rankovic, *Curr. Pharm. Des.* **2009**, *15*, 587–600.
- [13] A. Rampa, F. Belluti, S. Gobbi, A. Bisi, *Curr. Top. Med. Chem.* **2011**, *11*, 2716–2730.
- [14] R. León, A. G. Garcia, J. Marco-Contelles, *Med. Res. Rev.* **2013**, *33*, 139–189.
- [15] L. Piazzzi, A. Rampa, A. Bisi, S. Gobbi, F. Belluti, A. Cavalli, M. Bartolini, V. Andrisano, P. Valenti, M. Recanatini, *J. Med. Chem.* **2003**, *46*, 2279–2282.
- [16] L. Piazzzi, A. Cavalli, F. Belluti, A. Bisi, S. Gobbi, S. Rizzo, M. Bartolini, V. Andrisano, M. Recanatini, A. Rampa, *J. Med. Chem.* **2007**, *50*, 4250–4254.
- [17] L. Piazzzi, A. Cavalli, F. Colizzi, F. Belluti, M. Bartolini, F. Mancini, M. Recanatini, V. Andrisano, A. Rampa, *Bioorg. Med. Chem. Letters*. **2008**, *18*, 423–426.
- [18] G. L. Ellman, K. D. Courtney, V. Andres, R. M. Featherstone, *Biochem. Pharmacol.* **1961**, *7*, 88–95.
- [19] J. Cheung, M. J. Rudolph, F. Burshteyn, , M. S. Cassidy, E. N. Gary, J. Love, M. C. Franklin, J. J. Height, *J. Med. Chem.* **2012**, *55*, 10282–10286.
- [20] Schrodinger suite: <http://www.schrodinger.com/>
- [21] A. Rampa, A. Bisi, F. Belluti, S. Gobbi, P. Valenti, V. Andrisano, V. Cavrini, A. Cavalli, M. Recanatini, *Bioorg. Med. Chem.* **2000**, *8*, 497–506.

- [22] M. Recanatini, A. Cavalli, F. Belluti, L. Piazzzi, A. Rampa, A. Bisi, S. Gobbi, P. Valenti, V. Andrisano, M. Bartolini, V. Cavrini, *J. Med. Chem.* **2000**, *43*, 2007-2018.
- [23] Y. Nicolet, O. Lockridge, P. Masson, J.C. Fontecilla-Camps, F. Nachon, *J. Biol. Chem.* **2003**, *278*, 41141–41147.
- [24] H. Naiki, K. Higuchi, K. Nakakuki, T. Takeda, *Lab. Invest* **1991**, *65*, 104-110.
- [25] A. Rauk, *Dalton Trans* **2008**, *14*, 1273–1282.
- [26] Y. Porat, A. Abramowitz, E. Gazit, *Chem. Biol. Drug Des.* **2006**, *67*, 27–37.
- [27] E. Gazit, *FASEB J.* **2002**, *16*, 77–83.
- [28] H. Pajouhesh, R.G. Lenz, *NeuroRx* **2005**, *2*, 541–553.
- [29] M.C. Wenlock, R.P. Austin, P. Burton, A.M. Davis, P.D. Leeson, *J. Med. Chem.* **2003**, *46*, 1250–1256.
- [30] M. Bartolini, C. Bertucci, M. L. Bolognesi, A. Cavalli, C. Melchiorre, V. Andrisano, *ChemBioChem* **2007**, *8*, 2152-2161.
- [31] A. Tarozzi, M. Bartolini, L. Piazzzi, L. Valgimigli, R. Amorati, C. Bolondi, A. Djemil, F. Mancini, V. Andrisano, A. Rampa, *Pharmacol. Res. Perspect.* **2014**, Apr;2(2):e00023.
- [32] K. Vanommeslaeghe, E. P. Raman, A. D. MacKerell, Jr., *J. Chem. Inf. Model.* **2012**, *52*, 3155-3168.
- [33] T. Luhrs, C. Ritter, M. Adrian, D. Riek-Loher, B. Bohrmann, H. Doeli, D. Schubert, R. Riek, *Proc. Natl. Acad. Sci. USA* **2005**, *102*, 17342-17347.

- [34] S. A. Poulsen, A. A. Watson, D. P. Fairlie, D. J. Craik, *J. Struct. Biol.* **2000**, *130*, 142-152.
- [35] J. C. Phillips, R. Braun, W. Wang, J. Gumbart, E. Tajkhorshid, E. Villa, C. Chipot, R. D. Skeel, L. Kale, K. Schulten, *J. Comput. Chem.* **2005**, *26*, 1781-1802.
- [36] W. Humphrey, A. Dalke, K. Schulten, *J. Mol. Graph. Model.* **1996**, *14*, 33-38.
- [37] R. Kubo, M. Toda, N. Hashitsume, *Statistical Physics II: Nonequilibrium Statistical Mechanics*, Springer, **1991**.
- [38] J. Ryckaert, G. Ciccotti, H. Berendsen, *J. Comput. Phys.* **1977**, *23*, 327-341.